

# FOXO3a-modulated DEPDC1 promotes malignant progression of nephroblastoma via the Wnt/ $\beta$ -catenin signaling pathway

GENG GENG<sup>1</sup>, QINGHAO LI<sup>1</sup>, XINGQING GUO<sup>2</sup>, QINGBIN NI<sup>1</sup>, YONGTAO XU<sup>1</sup>,  
ZHAOLONG MA<sup>1</sup>, YONGJIN WANG<sup>1</sup> and MING MING<sup>1</sup>

<sup>1</sup>Department of Pediatric Surgery, Taian City Central Hospital, Taian, Shandong 271000;

<sup>2</sup>Department of Pediatric Respiriology and Cardiology, The Affiliated Hospital of Qingdao University, Qingdao 266000, P.R. China

Received February 28, 2022; Accepted April 27, 2022

DOI: 10.3892/mmr.2022.12788

**Abstract.** DEP domain containing 1 (DEPDC1) and forkhead box transcription factor 3a (FOXO3a) serve a role in tumor cells. To the best of our knowledge, however, the expression of DEPDC1 and FOXO3a in nephroblastoma and their role and potential mechanisms in nephroblastoma cells have not been reported. The aim of the present study was to characterize the expression of DEPDC1 and FOXO3a in nephroblastoma, as well as the underlying mechanisms. The expression levels of DEPDC1 and FOXO3a were detected using reverse transcription-quantitative PCR and western blotting. Cell viability, proliferation, invasion and migration were detected using Cell Counting Kit-8, colony formation, Transwell and wound healing assays, respectively. The activity of DEPDC1 promoter was detected by dual-luciferase reporter assay and the association between FOXO3a and DEPDC1 was detected using immunoprecipitation. DEPDC1 expression was significantly increased in nephroblastoma cells, particularly WiT49 cells. Compared with the negative control, DEPDC1 knockdown significantly inhibited proliferation, invasion and migration of WiT49 cells, while DEPDC1 overexpression (Ov) reversed these effects. By contrast, expression of FOXO3a was decreased in WiT49 cells and immunoprecipitation showed that FOXO3a bound to the DEPDC1 promoter. Ov-FOXO3a inhibited WiT49 cell proliferation, invasion and migration, as well as protein expression levels of phosphorylated-glycogen synthase kinase-3 $\beta$ , Wnt3a and  $\beta$ -catenin, while DEPDC1 Ov reversed the inhibitory effects of FOXO3a Ov on WiT49 cells. In conclusion, DEPDC1 promoted malignant progression of nephroblastoma via the Wnt/ $\beta$ -catenin signaling pathway; this may be regulated by FOXO3a.

## Introduction

Nephroblastoma, also known as Wilms' tumor, is the fourth most common malignant abdominal cancer in children and typically occurs between the ages of 3 and 5 years (1,2). Over the past 50 years, therapeutic options for patients with nephroblastoma have been primarily based on nephrectomy, complemented by radiotherapy, systemic chemotherapy and autologous stem cell transplantation (3). The improvement of treatment methods has led to long-term survival rate of >90% (4); thus nephroblastoma has one of the best prognoses among types of pediatric cancer. However, certain patients still experience poor prognosis due to cancer recurrence and metastasis (5). Therefore, discovering targeted biomarkers of nephroblastoma may contribute to understanding of the pathogenesis and metastatic mechanism and development of novel therapeutic strategies for management of patients with nephroblastoma.

DEP domain containing 1 (DEPDC1) is a tumor-associated gene (6,7) involved in regulation of cellular processes such as transcription, mitosis and apoptosis (8). In addition, other studies have shown that DEPDC1 participates in tumorigenesis and cancer progression in lung adenocarcinoma (9), gastric cancer (10), oral squamous cell carcinoma (11) and colorectal (12), liver (13) and breast cancer (14). By analyzing Therapeutically Applicable Research to Generate Effective Treatments database, Su *et al* (5) found that DEPDC1 is highly expressed in nephroblastoma and is associated with poor patient survival, indicating that DEPDC1 may serve as a potential prognostic and diagnostic biomarker for nephroblastoma. To the best of our knowledge, however, the role of DEPDC1 in the onset and development of nephroblastoma have not been investigated.

Forkhead box transcription factor O (FOXO), a subfamily of the forkhead transcription factor family, serves an essential role in cell function, including apoptosis, energy metabolism, DNA damage repair and oxidative stress (15-17). The FOXO subfamily includes four primary subtypes (FOXO1, FOXO3/FOXO3a, FOXO4 and FOXO6) that possess similar structure and function (18). The expression of FOXO4 is higher in skeletal muscle, while FOXO3a is primarily expressed in the brain, heart, kidney and spleen (19). FOXO6 is highly

---

*Correspondence to:* Dr Ming Ming, Department of Pediatric Surgery, Taian City Central Hospital, 29 Longtan Road, Taishan, Taian, Shandong 271000, P.R. China  
E-mail: mingming80S@126.com

**Key words:** nephroblastoma, DEP domain containing 1, forkhead box transcription factor 3a, proliferation, invasion, migration

expressed in nervous tissue (19). Studies have demonstrated that downregulation of the functioning of FOXO protein promotes tumorigenesis and cancer progression (20,21). In particular, FOXO3a, a tumor suppressor, has been reported to be associated with metastasis of malignant tumor, such as breast (22), pancreatic (23) and kidney cancer (24). A recent study found that FOXO3a inhibits nephroblastoma cell proliferation, migration and invasion and suppresses apoptosis by disrupting the Wnt/ $\beta$ -catenin signaling pathway (25). Downregulation of DEPDC1 also inhibits the Wnt/ $\beta$ -catenin signaling pathway (26). To the best of our knowledge, however, no report has studied the association between FOXO3a and DEPDC1 in onset and progression of nephroblastoma.

The aim of the present study was to clarify the association between DEPDC1 expression, prognosis of nephroblastoma and FOXO3a and associated signaling pathways to identify potential therapeutic targets.

## Materials and methods

**Cell culture and treatment.** Human normal renal (HK-2) and nephroblastoma cell lines (WiT49, WILTU-1 and GHINK-1) were obtained from American Type Culture Collection. All cell lines were cultured in DMEM supplemented with 10% FBS (both HyClone; Cytiva), 1% penicillin and 1% streptomycin (both from Beyotime Institute of Biotechnology) at 37°C with 5% CO<sub>2</sub>.

**Bioinformatics analysis.** JASPAR database (jaspar.genereg.net/) was used to predict the binding site of transcription factor FOXO3a to DEPDC1 promoter.

**Cell proliferation.** WiT49 cell (1x10<sup>5</sup> cells/well) proliferation was assessed by 5-ethynyl-2'-deoxyuridine (EdU) incorporation using a Click-iT™ EdU Imaging kit (cat. no. C10337; Thermo Fisher Scientific, Inc.) according to the manufacturer's protocol. Subsequently, 1  $\mu$ g/ml DAPI (Beyotime Institute of Biotechnology) was applied to stain the cells for 10 min at room temperature. Images were captured in five randomized fields of view using a confocal microscope.

**Cell transfection.** WiT49 cells (3x10<sup>5</sup> cells/well) were inoculated onto 6-well plates and cultured for 24 h at 37°C with 5% CO<sub>2</sub>. Following incubation, cells were transfected with overexpression (Ov)-DEPDC1, Ov-FOXO3a vector, negative control empty vector (Ov-NC), DEPDC1-targeting short hairpin (sh)RNA (sh-DEPDC1#1, and sh-DEPDC1#2) and sh-NC at a concentration of 25 nM. shRNA sequences are presented in Table I. All plasmids were synthesized by Shanghai GenePharma Co., Ltd. and transfected using Lipofectamine® 2000 (Invitrogen; Thermo Fisher Scientific, Inc.) according to the manufacturer's instructions. Blank control group cells were untreated. Following transfection for 48 h at 37°C, transfection efficiency was detected using reverse transcription-quantitative (RT-q)PCR and western blotting within 48 h.

**Cell counting kit-8 (CCK-8) assay.** CCK-8 assay was performed to assess cell viability. Briefly, WiT49 cells were seeded into a 96-well plate (6x10<sup>3</sup> cells/well) and incubated for

24, 48 and 72 h at 37°C under 5% CO<sub>2</sub>. Following incubation, 10  $\mu$ l CCK-8 solution (cat. no. P0037; Beyotime Institute of Biotechnology) was added to each well and cells were cultured for another 2 h at 37°C with 5% CO<sub>2</sub>. The optical density (OD) was measured at 450 nm using a microplate reader (BioTek Instruments, Inc.). Relative cell viability (%) was calculated as follows: (Treated OD<sub>A450</sub>-blank OD<sub>A450</sub>)/(control OD<sub>A450</sub>-blank OD<sub>A450</sub>) x100%.

**Colony formation assay.** WiT49 cells (5x10<sup>2</sup> cells/well) suspended in DMEM were inoculated into 6-well plates and incubated at 37°C in 5% CO<sub>2</sub> for 14 days. The cells were fixed with 70% ethanol at room temperature for 15 min, stained with 0.05% crystal violet at 37°C for 20 min and number of colonies was counted manually ( $\geq$ 50 cells) using an Olympus GX53 light microscope (Olympus Corporation; magnification, x4).

**Wound healing assay.** WiT49 cells were inoculated in 6-well plates (1x10<sup>5</sup> cells/well). When they reached 70-80% confluence, medium was replaced with serum-free DMEM (Shanghai Yimiao Chemical Technology Co., Ltd.) and cells were incubated overnight at 37°C at 5% CO<sub>2</sub>. Subsequently, a 200- $\mu$ l sterile pipette tip was used to scratch the cell monolayer. Following washing, with PBS three times, plates were maintained at 37°C with 5% CO<sub>2</sub>. Images were captured at 0 and 24 h using a BX51 inverted microscope (Olympus Corporation; magnification, x100) Cell migration (%) was calculated as follows: Final wound width/original wound width x100.

**Cell invasion assay.** Cell invasion ability was assessed using Matrigel-coated Transwell chambers (BD Biosciences). Briefly, 24-well Transwell plates (Corning, Inc.) with 8- $\mu$ m pore inserts were coated with Matrigel (BD Biosciences) at 37°C for 30 min. Next, 4x10<sup>4</sup> WiT49 cells were plated in serum-free DMEM (Shanghai Yimiao Chemical Technology Co., Ltd.). The upper chamber was precoated with Matrigel and cells were cultured in the upper chamber (0.1 ml cell suspension/well); the lower chamber was filled with DMEM (Shenzhen Baienwei Biotechnology Co., Ltd.) supplemented with 20% FBS. Following incubation at 37°C with 5% CO<sub>2</sub> for 24 h, the upper chamber was collected and cleaned. The invading cells were fixed with 4% formaldehyde at 25°C for 15 min and stained with 0.3% crystal violet solution (Sigma-Aldrich; Merck KGaA) at room temperature for 30 min. The invading cells were observed under a light microscope in five randomly selected fields of view (Olympus Corporation; magnification, x100).

**RT-qPCR.** Total RNA was extracted from WiT49 cells using RNazol RT (Sigma-Aldrich; Merck KGaA), according to the manufacturer's instructions. RNA concentration and quantification were assessed using a NanoDrop spectrophotometer (Thermo Fisher Scientific, Inc.). Following DNase I digestion, total RNA was reverse-transcribed into cDNA using a QuantiTect Reverse Transcription kit (Qiagen GmbH), according to the manufacturer's instructions. Subsequently, RT-qPCR was performed using a QuantiTect SYBR Green PCR kit (Qiagen GmbH), according to the manufacturer's instructions. The thermocycling conditions were as follows: Initial denaturation at 95°C for 10 min, followed by 40 cycles

Table I. shRNA and reverse transcription-quantitative PCR primer sequences.

Name	Sequence
sh-DEPDC1#1	5'-GGAAGTTGTCATAATTTAA-3'
sh-DEPDC1#2	5'-CGAGATGTATTCAGAACAA-3'
sh-NC	5'-TTCGGGTCATCCGATGGGCC-3'
DEPDC1	Forward: 5'-TCTGCCATGAAGTGCCTAGC-3' Reverse: 5'-TGATGTAGCCACAAACAACCAAA-3'
FOXO3a	Forward: 5'-GAGGAGGACGATGAAGACGAC-3' Reverse: 5'-TGTGCCGGATGGAGTTCTTC-3'
GAPDH	Forward: 5'-AGCCACATCGCTCAGACAC-3' Reverse: 5'-GCCCAATACGACCAATCC-3'

sh, short hairpin; DEPDC, DEP domain containing 1; FOXO3a, forkhead box transcription factor 3a; NC, negative control.

of 95°C for 10 sec and 60°C for 60 sec. Primers (GenScript) are listed in Table I. mRNA expression levels were quantified using the  $2^{-\Delta\Delta C_q}$  method (27) and normalized to the internal reference gene GAPDH.

**Western blotting.** WiT49 cells were washed twice with PBS, lysed with RIPA lysis buffer (Beyotime Institute of Biotechnology) and incubated for 30 min on ice. Cell lysate was centrifuged at 300 x g at 4°C for 20 min and protein supernatant was transferred into Eppendorf tubes. Total protein was quantified using a BCA protein assay kit (Bio-Rad Laboratories, Inc.). Following denaturation in a 95°C metal bath, Protein (20 µg/lane) was separated using 10% SDS-PAGE and transferred onto PVDF membranes (GE Healthcare), which were blocked with 10% skimmed milk for 1 h at room temperature. Subsequently, membranes were incubated overnight at 4°C with the primary antibodies (all 1:1,000; all Abcam) as follows: Anti-DEPDC1 (cat. no. ab197246), anti-FOXO3a (cat. no. ab109629), anti-phosphorylated (p-)glycogen synthase kinase-3β (GSK-3β; cat. no. ab75814), anti-GSK-3β (cat. no. ab93926), anti-Wnt3a (cat. no. ab219412), anti-β-catenin (cat. no. ab32572) and anti-GAPDH (cat. no. ab181602). Following incubation with primary antibodies, the membranes were incubated with goat anti-rabbit horseradish peroxidase-conjugated IgG secondary antibody (1:5,000; cat. no. ab150077; Abcam) at room temperature for 1 h. Protein bands were visualized using enhanced chemiluminescence reagent (GE Healthcare). Protein expression levels were semi-quantified using ImageJ software (version 1.46; National Institutes of Health) with GAPDH as the loading control.

**Dual-luciferase reporter assay.** WiT49 cells were inoculated in a 24-well plate (1x10<sup>5</sup> cells/well). When cells reached 80% confluence, luciferase activity was detected using the Promega Double Fluorescence Detection kit (Promega Corporation), according to the manufacturer's instructions. The DEPDC1 sequence including the putative binding sites of FOXO3a was sub-cloned and inserted into the pmirGLO vector (Promega Corporation) to construct DEPDC1-wild-type (WT) and mutant (MUT) reporter plasmids. 0.1 µg DEPDC1-WT or DEPDC1-MUT reporter plasmids containing Ov-FOXO3a

or Ov-NC were constructed (Shanghai GenePharma) to be co-transfected into WiT49 cells using Lipofectamine 2000 (Invitrogen; Thermo Fisher Scientific, Inc.). After 24 h, culture supernatant was discarded and collected cells were rinsed with PBS three times. Subsequently, 120 µl cell lysate was added to each well and shaken on a horizontal oscillator for 45 min at 50 x g. Next, 10 µl lysed cell mixture and 50 µl firefly luciferase reagent was added to a 1.5 ml tube and mixed. A total of 50 µl Stop/Glo Sealing Luciferase Reagent was added. Firefly/*Renilla* luciferase values were recorded and DEPDC1 promoter transfer activity was analyzed. The luciferase activity was also normalized to that of *Renilla*. Each group was set up in three wells and each experiment was repeated three times.

**Chromatin immunoprecipitation (ChIP)-PCR assay.** Total genomic DNA was isolated by 1 ml SDS (Beyotime) and sonicated using the EZChip™ kit (EMD Millipore). Cells (1x10<sup>7</sup>/ml) were sonicated for 10s on ice for 5 times and fragmented DNA was visualized on an agarose gel. For chromatin isolation, the sample was centrifuged at 15,000 x g for 10 min at 4°C to remove insoluble material and 10X ChIP dilution buffer was added to the collected supernatant. The sample was pre-cleared with protein G-agarose beads at 4°C for 1 h and pre-cleared chromatin was incubated with antibodies against FOXO3a (cat. no. ab70315; 3 µg/mg; Abcam) at 4°C overnight according to the manufacturer's protocol. Finally, PBS was adopted for the rinse of the sample. Immunochromatin was amplified using RT-qPCR as aforementioned.

**Statistical analysis.** Data are presented as the mean ± SD of ≥3 independent experiments. GraphPad Prism 8.0.2 software (GraphPad Software, Inc.) was used for data analysis. Statistical differences were determined using one-way ANOVA followed by Tukey's post hoc test for group comparisons. P<0.05 was considered to indicate a statistically significant difference.

## Results

*DEPDC1 is highly expressed in nephroblastoma cell lines and sh-DEPDC1 inhibits WiT49 cell proliferation.* Western blotting (Fig. 1A) and RT-qPCR (Fig. 1B) were used to

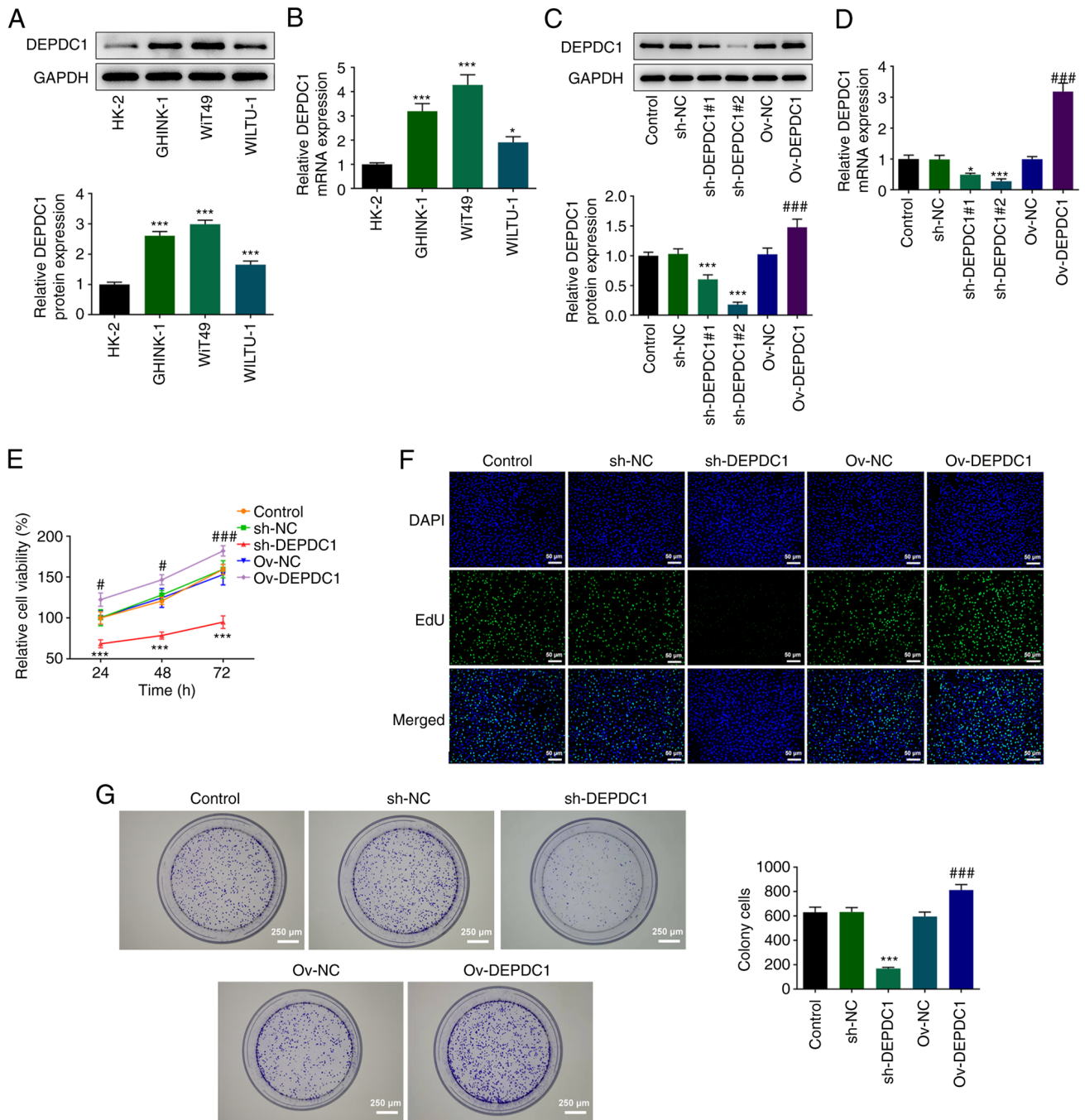


Figure 1. DEPDC1 is highly expressed in nephroblastoma cell lines and sh-DEPDC1 inhibits proliferation of WIT49 cells. (A) Western blotting and (B) reverse transcription-quantitative PCR were used to detect expression levels of DEPDC1 in WIT49 cells. (C) Protein and (D) mRNA expression of DEPDC1 in WIT49 cells following DEPDC1 overexpression or interference. (E) Cell Counting Kit-8 was used to detect cell viability. (F) EdU and (G) colony formation assay was used to detect cell proliferation. \* $P < 0.05$  and \*\*\* $P < 0.001$  vs. HK-2 or sh-NC; # $P < 0.05$  and ### $P < 0.001$  vs. Ov-NC. sh, short hairpin; DEPDC, DEP domain containing 1; FOXO3a, forkhead box transcription factor 3a; NC, negative control; Ov, overexpression.

detect DEPDC1 expression in nephroblastoma cell lines. Compared with normal renal cell line (HK-2), DEPDC1 expression was significantly increased in nephroblastoma cell lines (WIT49, WILTU-1 and GHINK-1), particularly WIT49 cells. Therefore, WIT49 cells were selected for subsequent experiments. To investigate the effects of DEPDC1 on nephroblastoma cell proliferation, DEPDC1 interference and overexpression plasmids were constructed and transfected into WIT49 cells. Compared with the control group, protein and mRNA expression levels of DEPDC1 in the Ov-DEPDC1

group significantly increased (Fig. 1C and D). In addition, transfection of interference plasmids significantly inhibited expression of DEPDC1, with sh-DEPDC1#2 exhibiting a greater interference efficiency than sh-DEPDC1#1. Therefore, sh-DEPDC1#2 was selected for subsequent experiments. CCK-8 assay results showed that sh-DEPDC1 significantly inhibited the viability of WIT49 cells. By contrast, DEPDC1 overexpression significantly increased cell viability (Fig. 1E). Proliferation of WIT49 cells was assessed using EdU incorporation (Fig. 1F) and colony formation experiments

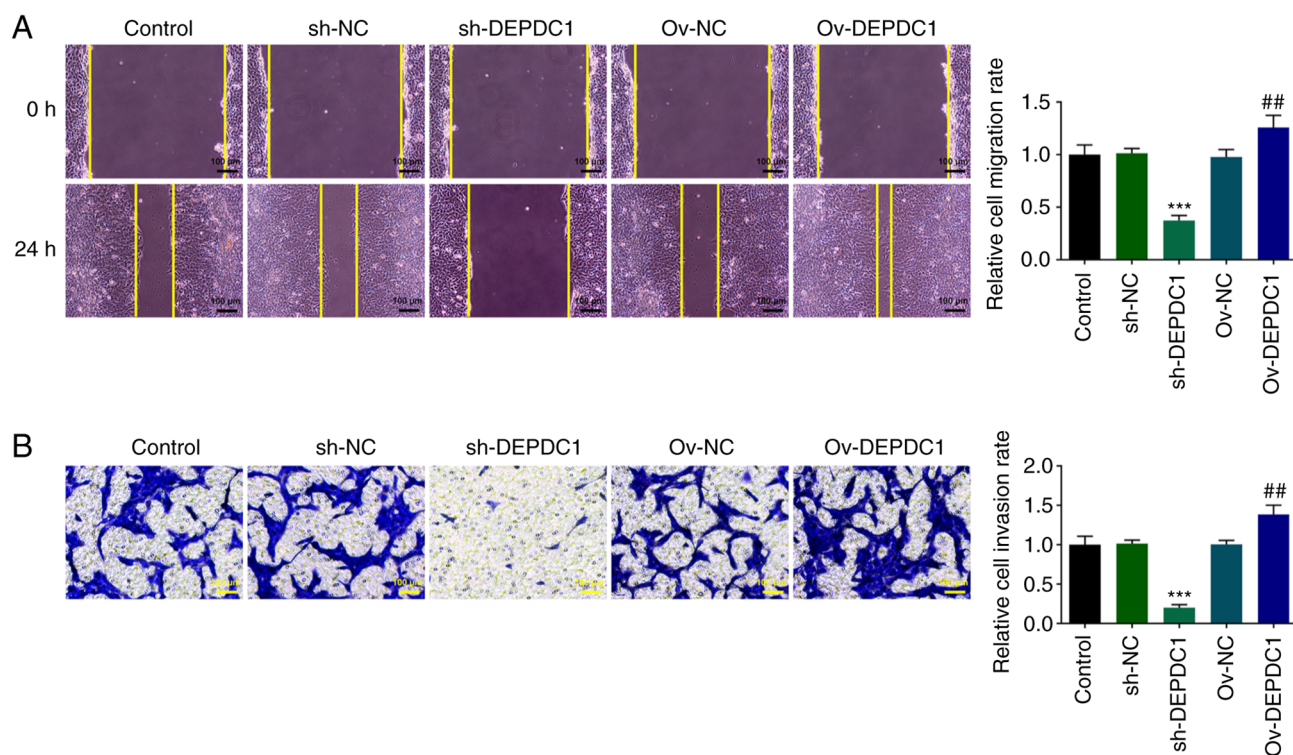


Figure 2. sh-DEPDC1 inhibits invasion and migration of nephroblastoma cells. (A) Wound healing and (B) Transwell assay were used to detect migration and invasion of nephroblastoma cells. \*\*\* $P < 0.001$  vs. sh-NC; \*\* $P < 0.01$  vs. Ov-NC. sh, short hairpin; DEPDC, DEP domain containing 1; NC, negative control; Ov, overexpression.

(Fig. 1G). sh-DEPDC1 inhibited cell proliferation compared with the control group, with the opposite results observed following DEPDC1 overexpression, evidenced by increased cell proliferation and tumorigenic ability in Ov-DEPDC1 group. These results indicated that DEPDC1 may promote nephroblastoma progression.

*sh-DEPDC1 inhibits nephroblastoma cell invasion and migration.* Wound healing (Fig. 2A) and Transwell (Fig. 2B) assay were used to detect cell invasion and migration. Compared with the Ov-NC group, cell migration and invasion in the Ov-DEPDC1 group significantly increased. In addition, sh-DEPDC1 significantly inhibited migration and invasion of WiT49 cells. These results suggested that DEPDC1 may promote invasion and migration of nephroblastoma cells.

*FOXO3a inhibits transcription of DEPDC1.* The binding sites of transcription factors FOXO3a and DEPDC1 promoter were predicted using JASPAR (Fig. 3A). Next, western blotting (Fig. 3B) and RT-qPCR (Fig. 3C) were performed to detect FOXO3a expression in WiT49 cells. FOXO3a mRNA and protein expression were significantly downregulated in WiT49 compared with HK-2 cells. Ov-FOXO3a plasmid was constructed to detect DEPDC1 promoter activity using luciferase assay. Protein and mRNA expression of FOXO3a were increased by overexpressing FOXO3a compared with that in Ov-NC (Fig. 3D and E). Ov-FOXO3a induced a significant decrease in luciferase activity in the presence of DEPDC1-WT promoter, while there was no significant change in the presence of MUT promoter (Fig. 3F). Subsequently,

binding of FOXO3a to DEPDC1 promoter was verified using ChIP. DEPDC1 has abundant enrichment in anti-FOXO3a in comparison with the IgG (Fig. 3G). Furthermore, DEPDC1 expression was significantly downregulated in Ov-FOXO3a nephroblastoma cells compared with Ov-NC group (Fig. 3H and I).

*FOXO3a mediates DEPDC1 promotion of malignant progression of nephroblastoma via Wnt/ $\beta$ -catenin signaling.* Considering the negative association between FOXO3a and DEPDC1 expression (Fig. 3H and I), DEPDC1 was overexpressed using Ov-FOXO3a to assess the effect of DEPDC1 on proliferation, migration and invasion of nephroblastoma cells and the potential mechanism. Compared with Ov-NC, Ov-FOXO3a significantly inhibited WiT49 cell viability, which was reversed by DEPDC1 overexpression, evidenced by the increased WiT49 cell viability in Ov-FOXO3a + Ov-DEPDC1 when compared with Ov-FOXO3a + Ov-NC group (Fig. 4A). EdU (Fig. 4B) and colony formation assay (Fig. 4C), which detected cell proliferation, showed that overexpression of DEPDC1 reversed inhibition of cell proliferation induced by Ov-FOXO3a in comparison with the Ov-FOXO3a + Ov-NC group. Wound healing (Fig. 4D) and Transwell assay (Fig. 4E) also showed that DEPDC1 overexpression reversed the inhibitory effect of Ov-FOXO3a on cell migration and invasion compared with Ov-FOXO3a + Ov-NC. Assessment of Wnt/ $\beta$ -catenin signaling pathway-associated protein expression levels (Fig. 5) showed that FOXO3a overexpression inhibited protein expression of p-GSK-3 $\beta$ , Wnt3a and  $\beta$ -catenin, while overexpression of DEPDC1 increased expression of the aforementioned proteins, suggesting that

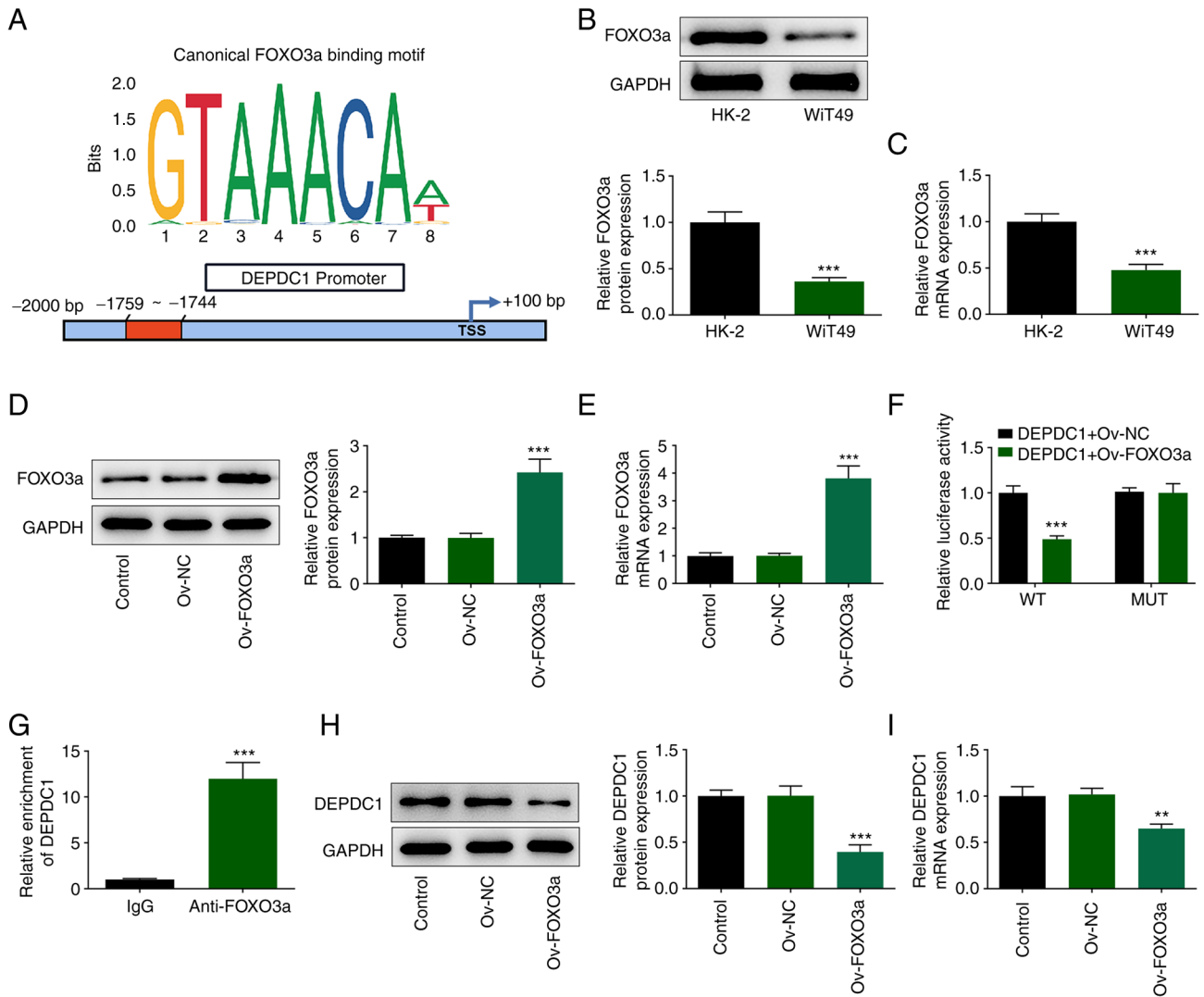


Figure 3. FOXO3a inhibits transcription of DEPDC1. (A) Binding site of transcription factor FOXO3a and DEPDC1 promoter. (B) Protein and (C) mRNA expression levels of FOXO3a were detected by western blotting and RT-qPCR, respectively. (D) Western blotting and (E) RT-qPCR were used to detect expression of FOXO3a in Ov-FOXO3a cells. (F) Luciferase detection of DEPDC1 promoter activity. (G) Immunoprecipitation indicated that FOXO3a bound to DEPDC1. (H) Western blotting and (I) RT-qPCR were used to detect expression of DEPDC1 in Ov-FOXO3a cells. \*\* $P < 0.01$  and \*\*\* $P < 0.001$  vs. HK-2 or Ov-NC. DEPDC, DEP domain containing 1; NC, negative control; Ov, overexpression; RT-q, reverse transcription-quantitative; WT, wild-type; MUT, mutant.

FOXO3a mediates DEPDC1-induced promotion of malignant progression of nephroblastoma via the Wnt/ $\beta$ -catenin signaling pathway.

## Discussion

Nephroblastoma typically occurs in children aged  $<5$  years and is one of the most common types of abdominal malignancy, accounting for 8% of all pediatric malignancy (28). Although the prognosis for patients with nephroblastoma has markedly improved over past decades, the mortality rate in 1969 to 1995 remained high in the USA (29). It is therefore important to determine the biological and molecular mechanisms underlying nephroblastoma progression.

The aberrant expression of DEPDC1, a recently identified tumor-associated gene, is associated with tumorigenesis in multiple types of cancer, such as lung adenocarcinoma (30), hepatocellular carcinoma (31) and gastric cancer (10) and contributes to cancer progression (7). The aberrant upregulation

of DEPDC1 has been observed in bladder (32) and breast cancer (33), multiple myeloma (34) and hepatocellular carcinoma (35), indicating its potential value as a therapeutic target. A recent study revealed that increased expression of DEPDC1 leads to poor survival in patients with nephroblastoma (36). Su *et al* (5) found that DEPDC1 is highly expressed in nephroblastoma and associated with poor survival using database network analysis. The present study investigated the role and underlying mechanism of DEPDC1 in nephroblastoma progression. DEPDC1 was highly expressed in nephroblastoma cells at both the protein and mRNA level. These results supported the hypothesis that high expression of DEPDC1 serves a carcinogenic role in nephroblastoma progression. To verify this, shRNA interference vectors were constructed to knock down DEPDC1 expression. Silencing expression of DEPDC1 significantly inhibited proliferation, migration and invasion of nephroblastoma cells. This is similar to results of Shen and Xi (37), who reported that DEPDC1 is highly expressed in lung adenocarcinoma and promotes tumor cell proliferation.

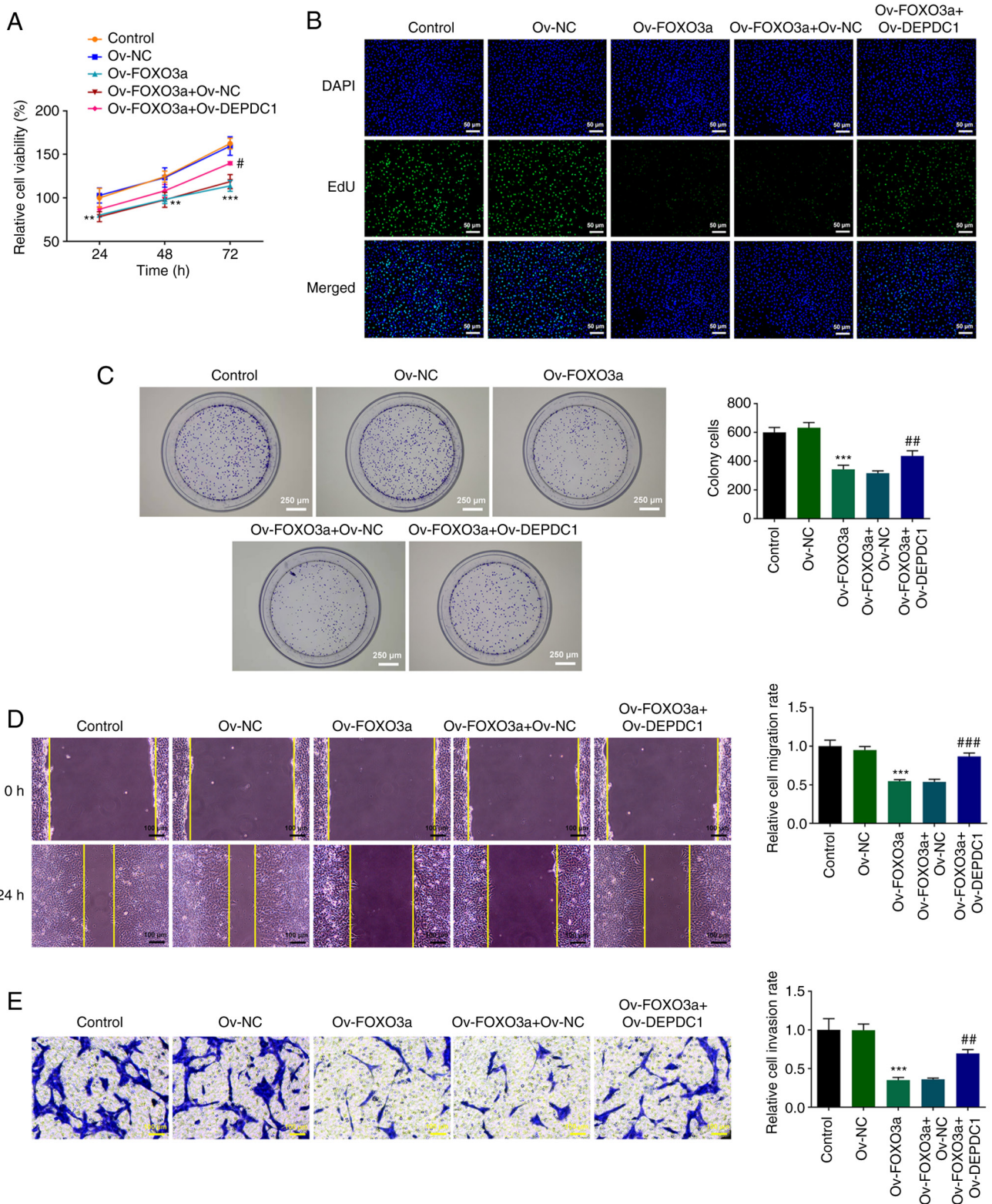


Figure 4. FOXO3a mediates DEPDC1-induced promotion of malignant progression of nephroblastoma. (A) Cell Counting Kit-8 assay was performed to detect cell viability. (B) EdU and (C) colony formation assay were used to test cell proliferation. (D) Wound healing and (E) Transwell assay were used to determine migration and invasion of WiT49 cells. \*\* $P < 0.01$  and \*\*\* $P < 0.001$  vs. Ov-NC; # $P < 0.05$ , ## $P < 0.01$  and ### $P < 0.001$  vs. Ov-FOXO3a + Ov-NC. DEPDC1, DEP domain containing 1; NC, negative control; Ov, overexpression; FOXO3a, forkhead box transcription factor 3a.

FOXO proteins are considered to be tumor suppressors due to their pro-apoptotic and anti-proliferative activity (17). Accumulating evidence indicates that suppressing the function of FOXO proteins promotes cancer progression and

tumorigenesis (20,38). FOXO3a, also known as FOXO3 or forkhead in rhabdomyosarcoma-like 1, is a key transcription factor regulating biological processes, including apoptosis, inflammation and DNA damage response (39-41) and is

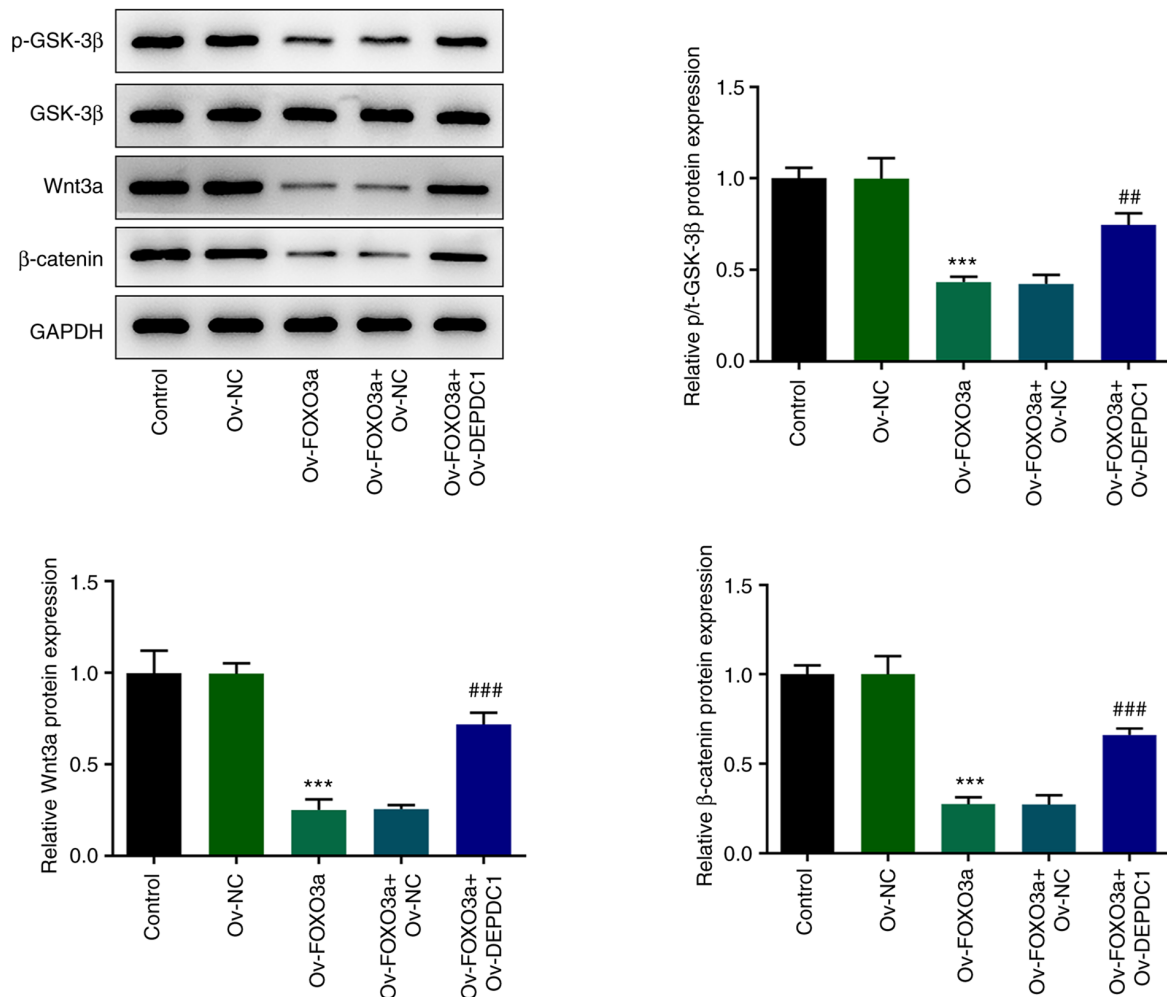


Figure 5. FOXO3a mediates DEPDC1-induced promotion of malignant progression of nephroblastoma via Wnt/ $\beta$ -catenin signaling. Expression levels of Wnt/ $\beta$ -catenin pathway-associated proteins (p-GSK-3 $\beta$ , Wnt3a and  $\beta$ -catenin) were detected by western blotting. \*\*\*\* $P$ <0.001 vs. Ov-NC; ## $P$ <0.01 and ### $P$ <0.001 vs. Ov-FOXO3a + Ov-NC. DEPDC, DEP domain containing 1; NC, negative control; Ov, overexpression; FOXO3a, forkhead box transcription factor 3a; p-, phosphorylated.

associated with extreme human longevity (18). As a tumor suppressor, FOXO3a exerts an inhibitory effect on cancer progression and is frequently inactivated in breast cancer cell lines (42). In the present study, expression of FOXO3a was downregulated in WiT49 cells compared with normal HK-2 cells; this is consistent with results of Qian and Liu (25).

JASPAR predicted that FOXO3a bound to and regulated DEPDC1, indicating an association between FOXO3a and DEPDC1 expression in nephroblastoma. In addition, co-immunoprecipitation results demonstrated that FOXO3a bound to DEPDC1 and Ov-FOXO3a decreased levels of DEPDC1. Ov-FOXO3a also prevented the promoting effect of Ov-DEPDC1 on proliferation, invasion and migration of nephroblastoma cells, indicating an association between FOXO3a and DEPDC1. Increasing evidence indicates that aberrant Wnt/ $\beta$ -catenin cascade leads to onset and progression of certain types of solid tumor and hematological malignancy (43,44). The Wnt signaling pathway is a key signal transduction pathway involved in renal development (45). The transcription factor  $\beta$ -catenin is a key component of the Wnt signaling pathway and its upregulation leads to occurrence of acute myeloid leukemia (46). Therefore, it may be important

to study the effect of abnormal Wnt/ $\beta$ -catenin signaling on the occurrence of nephroblastoma. In addition, DEPDC1 has been reported to activate the Wnt/ $\beta$ -catenin signaling pathway to regulate proliferation and metastasis of hepatocellular carcinoma cells (26,47). In the present study, FOXO3a overexpression decreased expression levels of p-GSK-3 $\beta$ ,  $\beta$ -catenin and Wnt3a protein, which are involved in the Wnt/ $\beta$ -catenin signaling pathway, and inhibited the DEPDC1-dependent Wnt/ $\beta$ -catenin pathway.

To the best of our knowledge, the present study is the first to investigate the role and mechanism of DEPDC1 in nephroblastoma. The present study only performed *in vitro* experiments; therefore, *in vivo* studies are needed to verify the results. DNMT1-mediated hypermethylation of the FOXO3a promoter downregulates FOXO3a expression in breast cancer (48). However, the mechanism underlying downregulation of FOXO3a expression and the effect of FOXO3a depletion on cell proliferation and DNA damage in nephroblastoma need further investigation. In addition, the association between signaling pathways other than Wnt/ $\beta$ -catenin (for example, NF- $\kappa$ B) and the mechanism of DEPDC1 in nephroblastoma need to be verified.



In conclusion, the present study demonstrated that DEPDC1 promoted malignant progression of nephroblastoma via the Wnt/ $\beta$ -catenin signaling pathway; this may be regulated by FOXO3a. The present findings suggested that DEPDC1 may serve as a valuable biomarker for understanding the mechanism of nephroblastoma progression.

### Acknowledgements

Not applicable.

### Funding

No funding was received.

### Availability of data and materials

The datasets used and/or analyzed during the current study are available from the corresponding author on reasonable request.

### Authors' contributions

GG, MM, QHL and XQG designed the study. QBN, YTX, ZLM and YJW performed the experiments. GG, MM, ZLM and YJW revised the manuscript. QHL, YTX and XQG collected and analyzed the data. ZLM, YJW and QBN confirm the authenticity of all the raw data. All authors have read and approved the final manuscript.

### Ethics approval and consent to participate

Not applicable.

### Patient consent for participation

Not applicable.

### Competing interests

The authors declare that they have no competing interests.

### References

- Xie W, Wei L, Guo J, Guo H, Song X and Sheng X: Physiological functions of Wilms' tumor 1-associating protein and its role in tumorigenesis. *J Cell Biochem*: Feb 12, 2019 (Epub ahead of print). doi: 10.1002/jcb.28402.
- Cone EB, Dalton SS, Van Noord M, Tracy ET, Rice HE and Routh JC: Biomarkers for Wilms tumor: A systematic review. *J Urol* 196: 1530-1535, 2016.
- Chakumatha E, Weijers J, Banda K, Bailey S, Molyneux E, Chagaluka G and Israels T: Outcome at the end of treatment of patients with common and curable childhood cancer types in Blantyre, Malawi. *Pediatr Blood Cancer* 67: e28322, 2020.
- Fuchs J: Surgical concepts in the treatment of Wilms tumor: An update. *Urologe A* 54: 1784-1791, 2015 (In German).
- Su C, Huang R, Yu Z, Zheng J, Liu F, Liang H and Mo Z: Myelin and lymphocyte protein serves as a prognostic biomarker and is closely associated with the tumor microenvironment in the nephroblastoma. *Cancer Med* 11: 1427-1438, 2022.
- Kanehira M, Harada Y, Takata R, Shuin T, Miki T, Fujioka T, Nakamura Y and Katagiri T: Involvement of upregulation of DEPDC1 (DEP domain containing 1) in bladder carcinogenesis. *Oncogene* 26: 6448-6455, 2007.
- Zhu Y, Sun L, Yu J, Xiang Y, Shen M, Wasan HS, Ruan S and Qiu S: Identification of biomarkers in colon cancer based on bioinformatic analysis. *Transl Cancer Res* 9: 4879-4895, 2020.
- Harada Y, Kanehira M, Fujisawa Y, Takata R, Shuin T, Miki T, Fujioka T, Nakamura Y and Katagiri T: Cell-permeable peptide DEPDC1-ZNF224 interferes with transcriptional repression and oncogenicity in bladder cancer cells. *Cancer Res* 70: 5829-5839, 2010.
- Li YY, Li W, Chang GZ and Li YM: Long noncoding RNA KTN1 antisense RNA exerts an oncogenic function in lung adenocarcinoma by regulating DEP domain containing 1 expression via activating epithelial-mesenchymal transition. *Anticancer Drugs* 32: 614-625, 2021.
- Gong Z, Chu H, Chen J, Jiang L, Gong B, Zhu P, Zhang C, Wang Z, Zhang W, Wang J, *et al*: DEPDC1 upregulation promotes cell proliferation and predicts poor prognosis in patients with gastric cancer. *Cancer Biomark* 30: 299-307, 2021.
- Guo J, Zhou S, Huang P, Xu S, Zhang G, He H, Zeng Y, Xu CX, Kim H and Tan Y: NNK-mediated upregulation of DEPDC1 stimulates the progression of oral squamous cell carcinoma by inhibiting CYP27B1 expression. *Am J Cancer Res* 10: 1745-1760, 2020.
- Wang Q, Jiang S, Liu J, Ma G, Zheng J and Zhang Y: DEP domain containing 1 promotes proliferation, invasion, and epithelial-mesenchymal transition in colorectal cancer by enhancing expression of suppressor of zest 12. *Cancer Biother Radiopharm* 36: 36-44, 2021.
- Guo W, Li H, Liu H, Ma X, Yang S and Wang Z: DEPDC1 drives hepatocellular carcinoma cell proliferation, invasion and angiogenesis by regulating the CCL20/CCR6 signaling pathway. *Oncol Rep* 42: 1075-1089, 2019.
- Zhao H, Yu M, Sui L, Gong B, Zhou B, Chen J, Gong Z and Hao C: High expression of DEPDC1 promotes malignant phenotypes of breast cancer cells and predicts poor prognosis in patients with breast cancer. *Front Oncol* 9: 262, 2019.
- Lam EW, Brosens JJ, Gomes AR and Koo CY: Forkhead box proteins: Tuning forks for transcriptional harmony. *Nat Rev Cancer* 13: 482-495, 2013.
- Gomes AR, Brosens JJ and Lam EW: Resist or die: FOXO transcription factors determine the cellular response to chemotherapy. *Cell Cycle* 7: 3133-3136, 2008.
- Farhan M, Wang H, Gaur U, Little PJ, Xu J and Zheng W: FOXO signaling pathways as therapeutic targets in cancer. *Int J Biol Sci* 13: 815-827, 2017.
- Calissi G, Lam EW and Link W: Therapeutic strategies targeting FOXO transcription factors. *Nat Rev Drug Discov* 20: 21-38, 2021.
- Chen YH, Li CL, Chen WJ, Liu J and Wu HT: Diverse roles of FOXO family members in gastric cancer. *World J Gastrointest Oncol* 13: 1367-1382, 2021.
- Jiramongkol Y and Lam EW: FOXO transcription factor family in cancer and metastasis. *Cancer Metastasis Rev* 39: 681-709, 2020.
- Yadav RK, Chauhan AS, Zhuang L and Gan B: FoxO transcription factors in cancer metabolism. *Semin Cancer Biol* 50: 65-76, 2018.
- Jin L, Zhang J, Fu HQ, Zhang X and Pan YL: FOXO3a inhibits the EMT and metastasis of breast cancer by regulating TWIST-1 mediated miR-10b/CADM2 axis. *Transl Oncol* 14: 101096, 2021.
- Zhao H, Chen W, Zhu Y and Lou J: Hypoxia promotes pancreatic cancer cell migration, invasion, and epithelial-mesenchymal transition via modulating the FOXO3a/DUSP6/ERK axis. *J Gastrointest Oncol* 12: 1691-1703, 2021.
- Ding D, Ao X, Li M, Miao S, Liu Y, Lin Z, Wang M, He Y and Wang J: FOXO3a-dependent Parkin regulates the development of gastric cancer by targeting ATP-binding cassette transporter E1. *J Cell Physiol* 236: 2740-2755, 2021.
- Qian C and Liu Q: FOXO3a inhibits nephroblastoma cell proliferation, migration and invasion, and induces apoptosis through downregulating the Wnt/ $\beta$ -catenin signaling pathway. *Mol Med Rep* 24: 796, 2021.
- Li Y, Tian Y, Zhong W, Wang N, Wang Y, Zhang Y, Zhang Z, Li J, Ma F, Zhao Z and Peng Y: *Artemisia argyi* essential oil inhibits hepatocellular carcinoma metastasis via suppression of DEPDC1 dependent Wnt/ $\beta$ -catenin signaling pathway. *Front Cell Dev Biol* 9: 664791, 2021.
- Sharifi A, Vahedi H, Honarvar MR, Amirani T, Nikniaz Z, Rad EY and Hosseinzadeh-Attar MJ: Vitamin D decreases CD40L gene expression in ulcerative colitis patients: A randomized, double-blinded, placebo-controlled trial. *Turk J Gastroenterol* 31: 99-104, 2020.

28. Al-Hussain T, Ali A and Akhtar M: Wilms tumor: An update. *Adv Anat Pathol* 21: 166-173, 2014.
29. Cotton CA, Peterson S, Norkool PA, Takashima J, Grigoriev Y, Green DM and Breslow NE: Early and late mortality after diagnosis of wilms tumor. *J Clin Oncol* 27: 1304-1309, 2009.
30. Wang W, Li A, Han X, Wang Q, Guo J, Wu Y, Wang C and Huang G: DEPDC1 up-regulates RAS expression to inhibit autophagy in lung adenocarcinoma cells. *J Cell Mol Med* 24: 13303-13313, 2020.
31. Zhou C, Wang P, Tu M, Huang Y, Xiong F and Wu Y: DEPDC1 promotes cell proliferation and suppresses sensitivity to chemotherapy in human hepatocellular carcinoma. *Biosci Rep* 39: BSR20190946, 2019.
32. Obara W, Ohsawa R, Kanehira M, Takata R, Tsunoda T, Yoshida K, Takeda K, Katagiri T, Nakamura Y and Fujioka T: Cancer peptide vaccine therapy developed from oncoantigens identified through genome-wide expression profile analysis for bladder cancer. *Jpn J Clin Oncol* 42: 591-600, 2012.
33. Hao S, Tian W, Chen Y, Wang L, Jiang Y, Gao B and Luo D: MicroRNA-374c-5p inhibits the development of breast cancer through TATA-box binding protein associated factor 7-mediated transcriptional regulation of DEP domain containing 1. *J Cell Biochem* 120: 15360-15368, 2019.
34. Kassambara A, Schoenhals M, Moreaux J, Veyrune JL, Rème T, Goldschmidt H, Hose D and Klein B: Inhibition of DEPDC1A, a bad prognostic marker in multiple myeloma, delays growth and induces mature plasma cell markers in malignant plasma cells. *PLoS One* 8: e62752, 2013.
35. Tian C, Abudoureyimu M, Lin X, Chu X and Wang R: Linc-ROR facilitates progression and angiogenesis of hepatocellular carcinoma by modulating DEPDC1 expression. *Cell Death Dis* 12: 1047, 2021.
36. Zheng H, Li BH, Liu C, Jia L and Liu FT: Comprehensive analysis of lncRNA-mediated ceRNA crosstalk and identification of prognostic biomarkers in Wilms' tumor. *Biomed Res Int* 2020: 4951692, 2020.
37. Shen J and Xi M: DEPDC1 is highly expressed in lung adenocarcinoma and promotes tumor cell proliferation. *Zhongguo Fei Ai Za Zhi* 24: 453-460, 2021 (In Chinese).
38. Liu Y, Ao X, Ding W, Ponnusamy M, Wu W, Hao X, Yu W, Wang Y, Li P and Wang J: Critical role of FOXO3a in carcinogenesis. *Mol Cancer* 17: 104, 2018.
39. Chen YF, Pandey S, Day CH, Chen YF, Jiang AZ, Ho TJ, Chen RJ, Padma VV, Kuo WW and Huang CY: Synergistic effect of HIF-1 $\alpha$  and FoxO3a trigger cardiomyocyte apoptosis under hyperglycemic ischemia condition. *J Cell Physiol* 233: 3660-3671, 2018.
40. Joseph J, Ametepe ES, Haribabu N, Agbayani G, Krishnan L, Blais A and Sad S: Inhibition of ROS and upregulation of inflammatory cytokines by FoxO3a promotes survival against *Salmonella typhimurium*. *Nat Commun* 7: 12748, 2016.
41. Fluteau A, Ince PG, Minett T, Matthews FE, Brayne C, Garwood CJ, Ratcliffe LE, Morgan S, Heath PR, Shaw PJ, *et al*: The nuclear retention of transcription factor FOXO3a correlates with a DNA damage response and increased glutamine synthetase expression by astrocytes suggesting a neuroprotective role in the ageing brain. *Neurosci Lett* 609: 11-17, 2015.
42. Zou Y, Tsai WB, Cheng CJ, Hsu C, Chung YM, Li PC, Lin SH and Hu MC: Forkhead box transcription factor FOXO3a suppresses estrogen-dependent breast cancer cell proliferation and tumorigenesis. *Breast Cancer Res* 10: R21, 2018.
43. Zhang Y and Wang X: Targeting the Wnt/ $\beta$ -catenin signaling pathway in cancer. *J Hematol Oncol* 13: 165, 2020.
44. Ashihara E, Takada T and Maekawa T: Targeting the canonical Wnt/ $\beta$ -catenin pathway in hematological malignancies. *Cancer Sci* 106: 665-671, 2015.
45. Hu Z, Li L, Cheng P, Liu Q, Zheng X, Peng F and Zhang Q: lncRNA MSC-AS1 activates Wnt/ $\beta$ -catenin signaling pathway to modulate cell proliferation and migration in kidney renal clear cell carcinoma via miR-3924/WNT5A. *J Cell Biochem* 121: 4085-4093, 2020.
46. Zhou J, Toh SH, Chan ZL, Quah JY, Chooi JY, Tan TZ, Chong PSY, Zeng Q and Chng WJ: A loss-of-function genetic screening reveals synergistic targeting of AKT/mTOR and WTN/ $\beta$ -catenin pathways for treatment of AML with high PRL-3 phosphatase. *J Hematol Oncol* 11: 36, 2018.
47. Qu D, Cui F, Lu D, Yang Y and Xu Y: DEP domain containing 1 predicts prognosis of hepatocellular carcinoma patients and regulates tumor proliferation and metastasis. *Cancer Sci* 110: 157-165, 2019.
48. Liu H, Song Y, Qiu H, Liu Y, Luo K, Yi Y, Jiang G, Lu M, Zhang Z, Yin J, *et al*: Downregulation of FOXO3a by DNMT1 promotes breast cancer stem cell properties and tumorigenesis. *Cell Death Differ* 27: 966-983, 2020.



This work is licensed under a Creative Commons Attribution-NonCommercial-NoDerivatives 4.0 International (CC BY-NC-ND 4.0) License.